Neurocomputing 151 (2015) 1171–1179

Contents lists available at ScienceDirect

Neurocomputing

journal homepage: www.elsevier.com/locate/neucom

Compressed sensing image reconstruction using intra prediction

Yun Song [a,b,*], Wei Cao [b], Yanfei Shen [c], Gaobo Yang [a]

[a] College of Computer Science and Electronic Engineering, Hunan University, Changsha 410082, China
[b] School of Computer and Communication Engineering, Changsha University of Science and Technology, Changsha 410014, China
[c] Institute of Computing Technology, Chinese Academy of Sciences, Beijing 100190, China

ARTICLE INFO

Article history:
Received 17 February 2014
Received in revised form
17 May 2014
Accepted 29 May 2014
Communicated by: D.-S. Huang
Available online 31 October 2014

Keywords:
Compressed sensing
Intra prediction
Image reconstruction
Postprocessing
Total variation

ABSTRACT

Compressed sensing (CS) provides a general signal acquisition framework that enables the reconstruction of sparse signals from a small number of linear measurements. In this article we present a CS image reconstruction algorithm using intra prediction method based on block-based CS image framework. The current reconstruction block is firstly predicted by its surrounding reconstructed pixels, and then its prediction residual will be reconstructed. Because the sparsity level of prediction residual is higher than its original image block, the performance of our proposed CS image reconstruction algorithm is significantly superior to the traditional CS reconstruction algorithm. Furthermore, total variation model is also used to suppress the blocking artifacts caused by intra prediction and measurement noise. Experimental results also show the competitive performance with respect to peak signal-to-noise ratio and subjective visual quality.

1. Introduction

Compressed sensing theory is an emerging framework that permits, under some conditions, compressible signals can be sampled at sub-Nyquist rates through non adaptive linear projection onto a random basis while enabling exact reconstruction at high probability [1,2]. Moreover, signals that can be well approximated by sparse representation, such as discrete cosine transform (DCT), wavelet transform or a trained dictionary, can be sensed at a much lower rate than double their actual bandwidth, as required by the Shannon-Nyquist sampling theory [3].

Compressed sensing (CS) theory mainly relies on two fundamental principles [4,5]: sparsity and incoherent. Let $x \in \mathbb{R}^n$ be an arbitrary compressible signal and let $\Psi = [\varphi_1, \cdots, \varphi_n]$ an sparse basis or dictionary in $\mathbb{R}^n$,

$$x = \sum_{i=1}^{n} \varphi_i \theta_i = \Psi \Theta \tag{1}$$

where $\Theta = [\theta_1, \cdots, \theta_n]^T$ is the vector of sparse coefficients that represent signal x on the basis Ψ. A signal is to be said sparse or compressible if most of the coefficients in Θ are zero or they can be discarded without much loss of information. Let $\Phi = [\phi_1, \cdots, \phi_N]^T$ be $M \times N$ measurement matrix, with $M \ll N$, such that $y = \Phi x$ is $M \times 1$ vector. This is an underdetermined function, that is to say, given the observation y, there are a number of x which can satisfy the equation $y = \Phi x$. However, CS theory states that if the measurement matrix Φ and sparse basis Ψ are incoherent and their product satisfies the Restricted Isometry Property (RIP) of order-k for all k-sparse vectors for a small isometry constant δ_k, that is,

$$(1-\delta_k)\|\Theta\|^2 \le \|\Phi\Psi\Theta\|^2 \le (1+\delta_k)\|\Theta\|^2 \tag{2}$$

The sparse coefficients Θ can be accurately reconstructed through the following constrained optimization problem [4]

$$\hat{\Theta} = \underset{\Theta}{\operatorname{argmin}} \|\Theta\|_{\ell_1} \ s.t. \quad y = \Phi\Psi\Theta \tag{3}$$

Afterwards, the signal x can be reconstructed by

$$\hat{x} = \Psi\hat{\Theta} \tag{4}$$

In most practical application, the signal x is not absolutely sparse or the measurements y may be corrupted by noise or quantization process. Then, the CS reconstruction procedure should be reformulated as

$$\hat{\Theta} = \underset{\Theta}{\operatorname{argmin}} \|\Theta\|_{\ell_1} \ s.t. \quad y - \|\Phi\Psi\Theta\|_{\ell_2} < \varepsilon \tag{5}$$

Based on the convex optimization theory [6], the optimization problem (5) can be solved by the following unconstrained Lagrangian formulation

$$\hat{\Theta} = \underset{\Theta}{\operatorname{argmin}} \lambda\|\Theta\|_{\ell_1} + (1/2)\|y - \Phi\Psi\Theta\|_{\ell_2}^2 \tag{6}$$

where λ is a regularization parameter which tradeoffs the sparsity level and the data fidelity. Typical methods for solving the problem in form (6) include basis pursuit denoising (BPDN) and gradient projection algorithms (GPSR) etc [7]. The final reconstruction signal is $\hat{x} = \Psi\hat{\Theta}$.

* Corresponding author.

http://dx.doi.org/10.1016/j.neucom.2014.05.088
0925-2312/

CS theory performs acquisition and compression simultaneously, and shifts almost all computation burdens to the decoder, resulting in a low-complexity encoder. It is very suitable for image or video application [8], where the computational resource and power is limited, such as low powerful wireless multimedia sensor network or handheld multimedia acquisition terminal [9]. In this article, we will investigate the CS reconstruction algorithm based on the observation that the sparsity level of prediction residual is higher than the original pixels, so the reconstruction performance with our proposed algorithm is improved as compared with the traditional ones.

In addition, CS theory can also be used as classification and recognition tools in computer vision, especially human face recognition and palmprint recognition [10–17]. Its basic idea is to cast recognition as a sparse representation problem through new mathematical tools from compressed sensing and L1 minimization.

The rest of the article is organized as follows. Section 2 introduces some classical CS reconstruction algorithms in image application domain. In Section 3, our proposed compressed sensing image reconstruction algorithm is described in detail, including the framework of our proposed algorithm, intra prediction mode and deblocking and denoising postprocessing. Section 4 presents the experimental results and conclusions are given in Section 5.

2. Compressed sensing for images

In recent years, there has been significant interest in compressed sensing theory for image application. The most well-known case is the so-called "single-pixel camera", which is a still image acquisition device developed by Rice University [17]. The most straightforward implementation of CS on 2D images is to recast the 2D array image as a 1D vector by some predefined scanning orders. For an $N \times$ N image, it will be formed a $N^2 \times 1$ vector. In this context, the sparsity transform Ψ is a $N^2 \times N^2$ matrix consisting of N^2 basis, the memory required to store this matrix grows very fast as the number of pixels in the image increases. In order to reduce the memory requirement, a block-based compressed sensing (BCS) framework was proposed in [18,19] for 2D images. That is, an image is divided into $B \times$ B non-overlapping blocks and every block is sensing measured independently. In this case, the sparsity matrix Ψ and sensing measurement matrix Φ for the whole image can also be written in a block-diagonal form as follows

$$\Psi = \begin{bmatrix} \varphi_B & & & \\ & \varphi_B & & \\ & & \ddots & \\ & & & \varphi_B \end{bmatrix} \quad \phi = \begin{bmatrix} \phi_B & & & \\ & \phi_B & & \\ & & \ddots & \\ & & & \phi_B \end{bmatrix} \tag{7}$$

The sensing measurement procedure for image block x_j is as follows

$$y_j = \phi_B x_j \tag{8}$$

where y_j is the measurement vector of image block x_j. In our proposed algorithm, the BCS framework is also used in the experiments due to its simplicity and high efficiency.

It is well known that the sparsity level of signal x decides the quality of reconstruction signal. In general, more sparsity signal x is, more high quality the reconstruction signal is. So as to improve the sparsity level of image signal, it is proposed that, instead of seeking sparsity in the image transform domain, the total variation (TV) model is used in CS image reconstruction in [20] as follows

$$\hat{x} = \underset{x}{\arg\min}\ ||x||_{TV} + \lambda ||y - \Phi x||_2 \tag{9}$$

However, the TV model possesses some undesirable properties, such as the staircase effect.

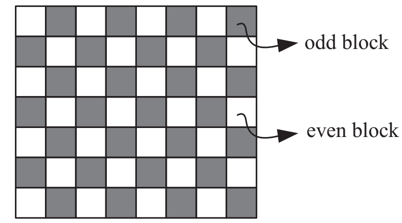

Fig. 1. Non-overlapping image blocks in checkerboard pattern.

In this article the sparsity level of reconstruction image will be enhanced by our proposed intra prediction algorithm which will be detailed in the next section. Based on the traditional image coding theory, if the current image block can be efficiently predicted, the prediction residual can be more compressed than the original image block in some transform domains [21,22], such as DCT. In other words, the sparsity level of prediction residual is higher than original block.

Let x_{pred_j} be the prediction of image block x_j, the compressed sensing measurement of its prediction residual is

$$y_{resi_j} = \phi_B \left(x_j - x_{pred_j} \right) = \phi_B x_{resi_j} \tag{10}$$

That is

$$y_{resi_j} = y_j - \phi_B\, x_{pred_j} \tag{11}$$

If the best prediction x_{pred_j} can be found, the prediction residual x_{resi_j} can also be accurately reconstructed through y_{resi_j} and the final reconstruction result $\hat{x}_j$ is calculated by $\hat{x}_j = x_{pred_j} + x_{resi_j}$. Because the prediction residual x_{resi_j} is much sparser than the original image x_j, the reconstruction accuracy of image block x_j is also higher.

3. Proposed CS image reconstruction algorithm

3.1. Framework of our proposed CS image reconstruction algorithm

In our proposed method, the image is divided into non-overlapping blocks for compressed sensing measurement as the above BCS framework. Although every image block x_j can be reconstructed by the measurement vector y_j independently based on the general sparsity basis DCT or DWT, the quality of reconstruction image can be further improved by integrating our proposed intra prediction in the reconstruction procedure, as shown in Fig. 1.

In traditional video coding standard, such as H.264/AVC [22], intra prediction is an important coding tool to improve the compression efficiency. Its basic idea is to use reconstructed pixels, including the left and the above neighbor pixels, to predict the current coding block, and finally the best prediction mode is selected by rate distortion optimization (RDO) theory. However, the original image block is not available in the CS reconstruction procedure, so it is impossible to directly select the best prediction mode in original pixel domain by RDO theory. In our proposed method, the best intra prediction mode is selected in compressed sensing domain. Let $x^k_{pred_j}$ be prediction block by the *kth* prediction mode and $\hat{x}_j$ is the reconstruction block by straightforward reconstruction algorithm, the best mode *kb* is selected by the following function

$$kb = \min_k \left|\left| x^k_{pred_j} - \hat{x}_j \right|\right|^2 \tag{12}$$

Algorithm 1. Compressed Sensing Image Reconstruction

Require: ϕ_B, Y
Output: X

1. Recover the every image block x_j based on the observed value Y based on some predefined sparsity basis through some optimization algorithm, such as BPDN or GPSR, $\hat{x}_j$ represents the corresponding recovery value.
2. Predict the odd image block x_j by its surrounding pixels in checkerboard pattern and its prediction value is denoted by $x^k_{\text{pred}_j}$, where k is the number of prediction modes.
3. Select the best prediction mode based on the function (12), let *kb* be the best selected prediction mode.
4. Measure the prediction image block $x^{kb}_{\text{pred}_j}$, and calculate the $y_{\text{resi}_j} = y_j - \phi_B x^{kb}_{\text{pred}_j}$
5. Recover the prediction residual x_{resi_j}.
6. Reconstruct the image block by $\hat{x}_j = x^{kb}_{pred_j} + x_{resi_j}$
7. Reconstruct the even image blocks in the same step 2–6.
8. Output recovery image X

Once the best prediction mode has been selected, then the best prediction block $x^{kb}_{\text{pred}_j}$ will be measured by sensing matrix ϕ_B and the y_{resi_j} is achieved by equation (11). Finally the image block *j* can be reconstructed based on the previous description as follows

$$\hat{x}_j = x^{kb}_{pred_j} + x_{resi_j} \tag{13}$$

To improve the intra prediction accuracy, the current reconstruction block will be predicted by its surrounding pixels, not only the left and above neighbor pixels as used in H.264/AVC video coding standard. As shown in Fig. 2, the surrounding neighbor pixels in the gray region will be used to predict the central image block, the detailed intra prediction method will be specified in the next subsection. It notes that, in order to assure the surrounding pixels available when the current block is reconstructed, the order of recovery image block takes on checkerboard arrangement instead of traditional horizontal raster scanning pattern, as shown in Fig. 1. The white image block is firstly reconstructed by some classical straightforward reconstruction algorithms based on DCT or DWT sparsity basis, then the gray block is predicted by our proposed new intra prediction algorithm and the prediction residual is reconstructed by ℓ_1 optimization method, the final reconstructed gray image block is achieved by adding the reconstruction prediction residual to the prediction block. After the gray is reconstructed, it will be used to predict and reconstruct the white image block in the same manner iteratively. Algorithm 1 shows the detailed reconstruction process for block-based compressed sensing image.

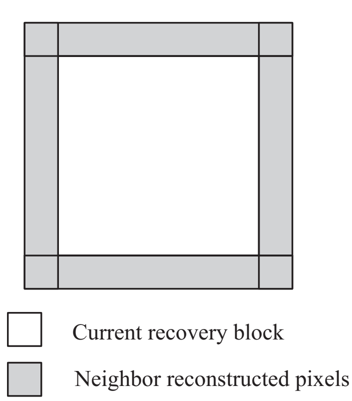

Fig. 2. Current reconstruction block and its neighbor pixels.

3.2. Intra prediction mode

In our proposed algorithm, intra prediction will be used to improve the performance of CS image reconstruction by exploiting the inter pixel correlation. Because the reconstruction order of image blocks in our proposed algorithm takes on checkerboard fashion, the current image block can be predicted by its surrounding reconstructed pixels, rather than the left and above neighbor pixels used in H.264/AVC video coding standard. The prediction accuracy can also be further boosted since more available neighbor pixels are involved into the prediction procedure. In this article, there are total five prediction modes designed for intra prediction, including horizontal prediction, vertical prediction, DC prediction, left-down-diagonal prediction, and right-down-diagonal prediction, as shown in Fig. 3. Of course, there may be more intra prediction modes which can be integrated into our proposed image reconstruction algorithm.

3.2.1. Horizontal prediction

In the horizontal prediction mode, the predicted pixel is obtained by weighted average from left pixel PL and right pixel PR in the same row, as follows

$$P = PL \times (1 - dx) + PR \times dx \tag{14}$$

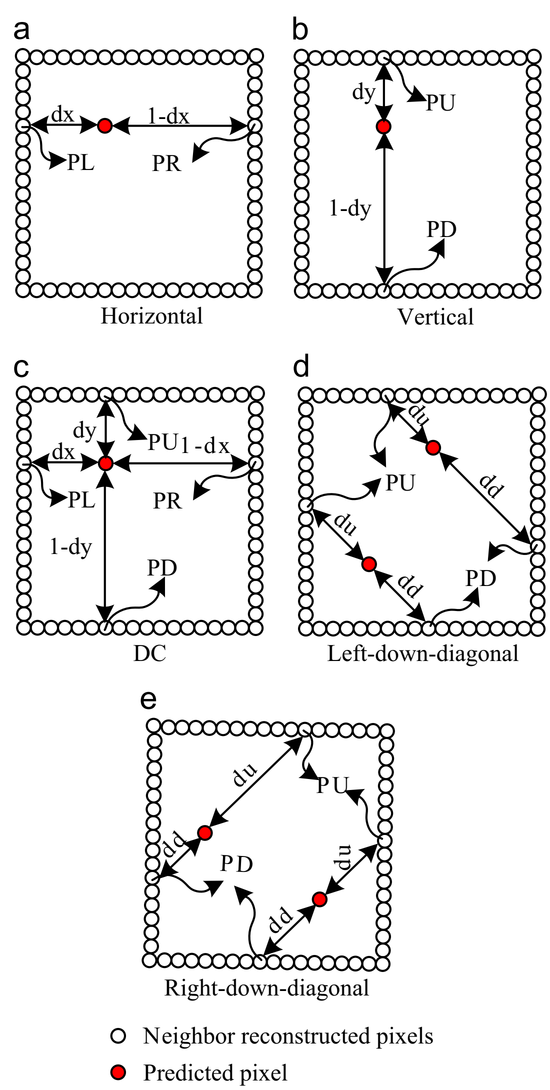

Fig. 3. Intra prediction modes and its neighbor pixels.

where dx and $1-dx$ are the relative distance from the predicted pixel to left and right neighbor reconstructed pixels, as shown in Fig. 3(a).

3.2.2. Vertical prediction

In the vertical prediction mode, the predicted pixel is obtained by weighted average from up pixel PU and down pixel PD in the same column, as follows

$$P=PU\times(1-dy)+PD\times dy \tag{15}$$

where dy and $1-dy$ are the relative distance from the predicted pixel to up and down neighbor reconstructed pixels, as shown in Fig. 3(b).

3.2.3. DC prediction

In the DC prediction mode, the predicted pixel is obtained by weighted average from four directional neighbor pixels PL, PR, PU, and PD as follows

$$P=(PU\times(1-dy)+PD\times dy+\ PL\times(1-dx)+PR\times dx)/2 \tag{16}$$

where variables dx and dy have the same interpretation as horizontal and vertical prediction mode, as shown in Fig. 3(c).

3.2.4. left-down-diagonal prediction

In the left-down-diagonal prediction mode, the predicted pixel is obtained by weighted average of two pixels which locate in the same left-down-diagonal with the predicted pixel, as shown in Fig. 3(d). It is calculated as follows

$$P=PU\times du+PD\times dd \tag{17}$$

3.2.5. Right-down-diagonal prediction

In the right-down-diagonal prediction mode, the predicted pixel is obtained by weighted average of two pixels which locate in the same right-down-diagonal with the predicted pixel, as shown in Fig. 3(e). The calculation method is the same as the left-down-diagonal prediction mode.

3.3. Deblocking and denoising

To eliminate the blocking artifacts caused by intra prediction in Section 3.2 and reconstruction noise caused by measurement error, the Rudin-Osher-Fatemi (ROF)/Total Variation (TV) model is used in our proposed CS reconstruction algorithm. For a 2-D image signal $u\in R^{m\times n}$, the total variation is defined by

$$||u||_{TV}=\left|\left|\frac{\partial u}{\partial x}\right|\right|_1+\left|\left|\frac{\partial u}{\partial y}\right|\right|_1 \tag{18}$$

The TV model corresponds to solve the following optimization problem,

$$\min_u ||u||_{TV}+\frac{\mu}{2}||u-f||_2 \tag{19}$$

where f is the reconstruction image in Section 3.1.

Due to the non-differentiability and non-linearity of the TV term in problem (19), this problem is computationally challenging to solve despite of its simple form. Hence, much effort has been devoted to devise an efficient algorithm to solve it [25]. Here we will apply the split bregman algorithm to solve problem (19).

We will denote $\partial u/\partial x$ by u_x and $\partial u/\partial y$ by u_y, the problem (19) is equal to the following constrained optimization problem

$$\min_u \left|\left|d_x\right|\right|_1+\left|\left|d_y\right|\right|_1+\frac{\mu}{2}||u-f||_2 \quad s.t.\quad d_x=u_x \quad and \quad d_y=u_y \tag{20}$$

With Lagrangian formulation, the constrained optimization problem can be relaxed to the following unconstrained optimization problem

$$\min_{u,d_x,d_y}\left|\left|d_x\right|\right|_1+\left|\left|d_y\right|\right|_1+\frac{\mu}{2}\left|\left|u-f\right|\right|_2+\frac{\lambda}{2}\left|\left|d_x-u_x\right|\right|_2+\frac{\lambda}{2}||d_y-u_y||_2 \tag{21}$$

where $\lambda>0$ is a constant.

By using the split bregman algorithm, we can thus solve (21) as follows

$$\begin{aligned}(u^{k+1},d_x^{k+1},d_y^{k+1})=\min_{u,d_x,d_y}&\left|\left|d_x\right|\right|_1+\left|\left|d_y\right|\right|_1+\frac{\mu}{2}||u-f||_2\\&+\frac{\lambda}{2}\left|\left|d_x-u_x-b_x^k\right|\right|_2+\frac{\lambda}{2}\left|\left|d_y-u_y-b_y^k\right|\right|_2\end{aligned} \tag{22}$$

where the superscript k is the iteration number and the proper values of b_x^k and b_y^k are updated through bregman iteration as follows

$$b_x^{k+1}=b_x^k+\left(u_x^{k+1}-d_x^{k+1}\right) \tag{23}$$

$$b_y^{k+1}=b_y^k+\left(u_y^{k+1}-d_y^{k+1}\right) \tag{24}$$

It is noted that problem (22) is smooth with respect to u, therefore, to solve this optimization problem, we can simply set its variation derivative equal to zero

$$\mu\left(u^{k+1}-f\right)-\lambda\nabla_x^T\left(d_x^k-u_x^{k+1}-b_x^k\right)-\lambda\nabla_y^T\left(d_y^k-u_y^{k+1}-b_y^k\right)=0 \tag{25}$$

that is

$$(\mu I+\lambda\Delta)u^{k+1}=\mu f+\lambda\nabla_x^T\left(d_x^k-b_x^k\right)+\lambda\nabla_y^T\left(d_y^k-b_y^k\right) \tag{26}$$

In order to achieve optimal efficiency, we solve the system of equations using the Gauss-Seidel method. The Gauss-Seidel solution

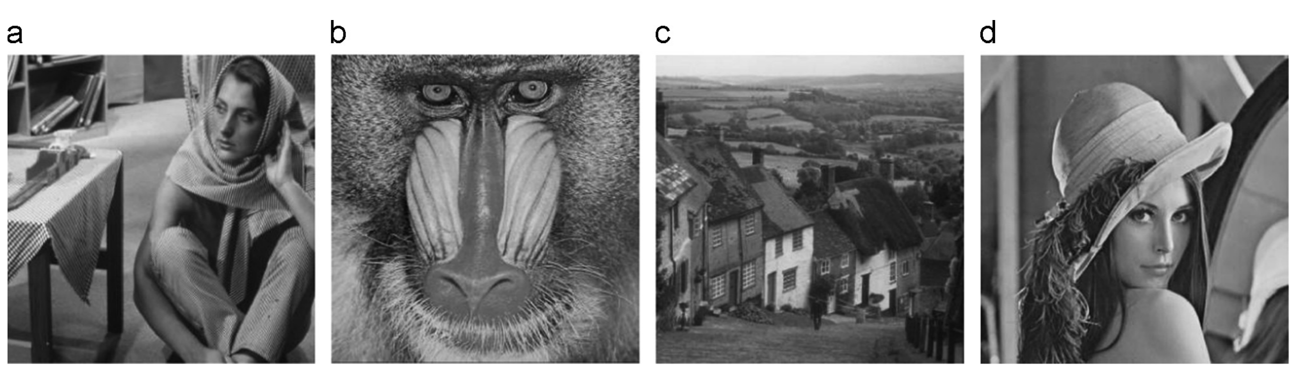

Fig. 4. Test images used in our experiments.

can be written component-wise as $u_{i,j}^{k+1} = G_{i,j}^{k}$ where

$$G_{i,j}^{k} = \frac{\lambda}{\mu+4\lambda}\Big(u_{i+1,j}^{k} + u_{i-1,j}^{k} + u_{i,j+1}^{k} + u_{i,j-1}^{k}$$

$$+ d_{x,i-1,j}^{k} - d_{x,i,j}^{k} + d_{y,i,j-1}^{k} - d_{y,i,j}^{k} - b_{x,i-1,j}^{k}$$

Fig. 5. Straightforward reconstruction of odd image blocks.

Fig. 6. Even image blocks predicted by intra prediction method at the sampling ratio of 0.8.

$$+ b_{x,i,j}^{k} - b_{y,i,j-1}^{k} + b_{y,i,j}^{k}\Big) + \frac{\mu}{\mu+4\lambda} f_{i,j} \tag{27}$$

At the boundaries of reconstruction image, one-sided finite differences are used instead of the centered finite differences.

Because there is no coupling between d and u in the problem (22), we can explicitly compute the optimal value of d_x and d_y using shrinkage operators as follows

$$d_x^{k+1} = shrink\left(u_x^{k+1} + b_x^{k}, \frac{1}{\lambda}\right) \tag{28}$$

$$d_y^{k+1} = shrink\left(u_y^{k+1} + b_y^{k}, \frac{1}{\lambda}\right) \tag{29}$$

where

$$shrink(x,\gamma) = \frac{x}{|x|}\max(|x|-\gamma, 0) \tag{30}$$

This shrinkage is extremely fast, and requires only a few operations per element.

In summary, the proposed CS reconstruction algorithm mainly consists of two steps:

Step1: Reconstruct the image X from block compressed sensing measurements Y using intra prediction algorithm as Algorithm 1;

Table 1
The PSNR performance of compressed sensing image reconstruction (unit: dB).

Image	Algorithm	Sampling ratio					
		0.3	0.4	0.5	0.6	0.7	0.8
Lena	BPDN	28.14	30.46	32.20	33.47	34.03	34.88
	BPDN_IP	28.79	30.86	32.60	34.04	36.19	38.55
	GPSR	28.11	30.45	32.19	33.47	34.03	34.88
	GPSR_IP	28.59	30.36	32.21	33.84	35.07	36.41
Barbara	BPDN	25.39	27.41	29.08	30.73	32.13	32.80
	BPDN_IP	25.63	27.84	29.25	30.12	32.56	35.30
	GPSR	25.48	27.37	29.34	30.84	32.19	32.96
	GPSR_IP	25.10	27.26	29.28	31.12	32.92	34.28
Mandirll	BPDN	20.78	21.72	23.33	24.67	26.15	27.66
	BPDN_IP	20.55	21.74	23.31	24.68	26.32	27.97
	GPSR	20.63	21.91	23.24	24.70	26.21	27.60
	GPSR_IP	20.63	22.03	23.28	24.67	26.31	28.04
Goldhill	BPDN	27.38	28.79	30.40	31.77	32.52	33.66
	BPDN_IP	27.28	29.13	30.56	31.90	33.23	34.58
	GPSR	27.32	29.13	30.41	31.65	32.54	33.71
	GPSR_IP	27.42	29.03	30.61	31.97	33.32	34.52

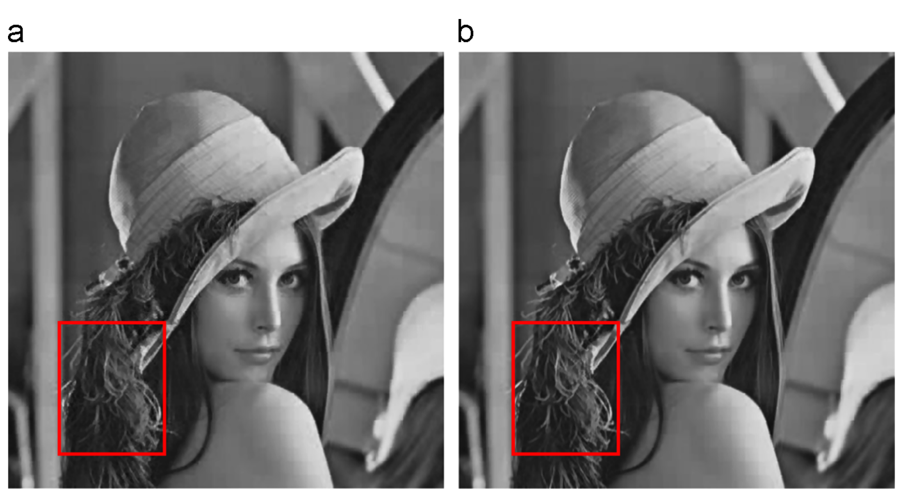

Fig. 7. The reconstruction images of lena test image at the sampling ratio of 0.8.

Step2: Suppress the blocking artifacts and reconstruction noise by TV model.

4. Experimental results

In this section, we will report the experimental results of our proposed compressed sensing image reconstructed algorithm with intra prediction, which is implemented on MATLAB platform. Throughout, several popular grayscale images of size 512×512 [23] are employed in our experiments, such as barbara, mandrill, goldhill, and lena, as shown in Fig. 4. We use BCS framework with non-overlapping image blocks of size 16×16. In all cases, the images are subjected to a BCS measurement process with ϕ_B in (7) which is an orthonormalized dense Gaussian matrix and the sparsity basis is 16×16 DCT transform. In order to validate the effectiveness of our proposed algorithm, every image is measured in different sampling ratios. It also notes that the measurement side in CS image applications does not need do any modification as the traditional straightforward CS reconstruction algorithm for images in our proposed reconstruction algorithm.

The objective quality of the reconstruction images was measured in terms of a peak signal-to-noise ratio (PSNR) between the reconstruction image and original images, which is computed as

Fig. 8. Comparison of subject quality for reconstruction images at the sampling ratio of 0.3. The top line: the reconstruction images with postprocessing model. The bottom line: the reconstruction images without postprocessing model.

Fig. 9. Local details for barbara reconstruction image at the sampling ratio of 0.3. The top line: the reconstruction images with postprocessing model. The bottom line: the reconstruction images without postprocessing model.

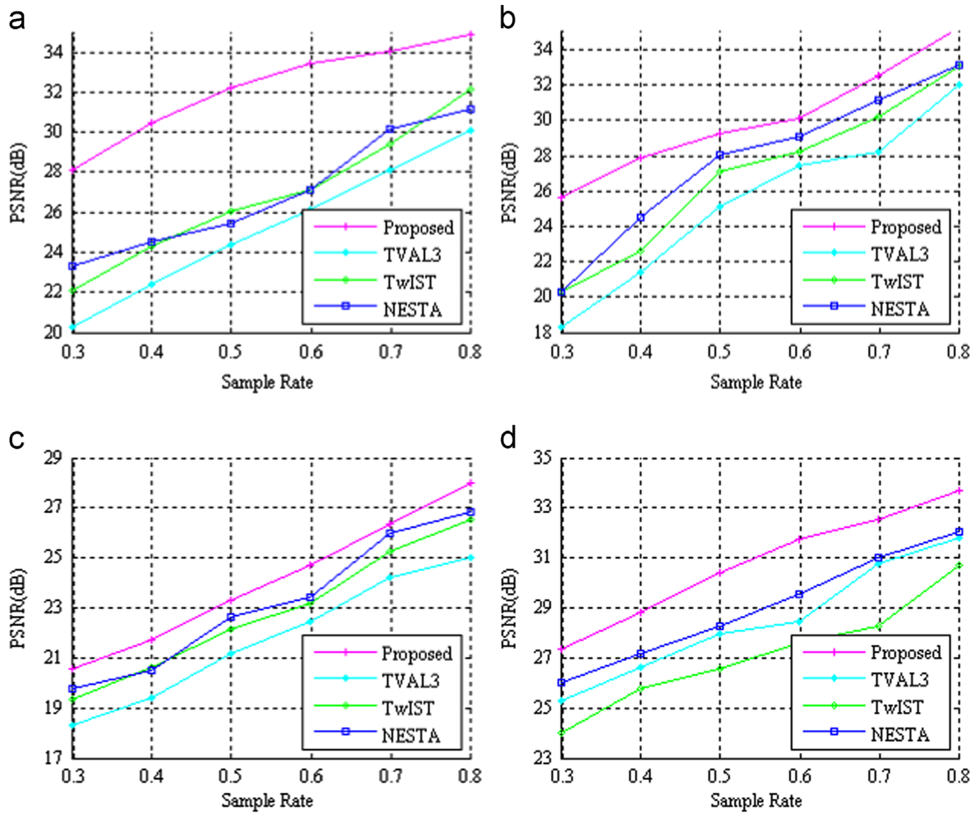

Fig. 10. PSNR comparison of four CS reconstruction algorithms with six sampling ratios.

the following expression:

$$PSNR = 10\log_{10}\frac{255^2}{(1/mn)\sum_{i=1}^{mn}(\hat{x}_i - x_i)^2} \tag{31}$$

where the $\hat{x}_i$ and x_i denote the pixel value of the reconstruction image and original image respectively; m and n denote the width and the height of the test images.

The solvers for straightforward CS reconstruction include BPDN and GPSR [24], which are also used to reconstruct prediction residues in our proposed algorithm, denoted by BPDN_IP and GPSR_IP respectively. In all cases, the sparsity basis is 16×16 DCT orthogonal transform.

Firstly, the odd image blocks are straightforwardly reconstructed, as shown in Fig. 5. The black image blocks will be predicted by our proposed intra prediction method using its surrounding reconstructed pixels. It notes that the blocks located at the image boundary are always straightforwardly reconstructed.

The predicted even image blocks by our proposed intra prediction method are illustrated in Fig. 6 at the sampling ratio of 0.8. It shows that the even image blocks can be efficiently predicted by its surrounding reconstructed pixels although there are some obvious artifacts at the block edge.

The final images of straightforward reconstruction method and our proposed reconstruction method with intra prediction by BPDN recovery algorithm at the sampling ratio of 0.8 are shown in Fig. 7. It can be seen that there are much distortion in the straightforward reconstruction images, especially in the complex texture image region, which is labeled in rectangle in Fig. 7.

The PSNR performance for test reconstruction images is detailed in Table1. In order to evaluate our proposed method comprehensively, different sampling ratios are tested from 0.3 to 0.8. We can find that the improved performance at the high sampling ratio is more than at the low sampling ratio. The major reason is that the reconstruction pixels at high sampling ratio used in intra prediction is more accurate than at low sampling ratio and can provide exact prediction for the predicted blocks. In addition, there are differences in reconstruction performance for different test images; the achieved gain for test images with complex texture is less than the others, such as mandrill test image, even in few worst cases, the performance of our proposed reconstruction method is lower than the straightforward reconstruction method, because it is very difficult for intra prediction method to predict texture image blocks only using our proposed five intra prediction modes. Its performance can be further improved if more intra prediction modes are adopted.

To further evaluate the performance of our proposed postprocessing method described in Section 3.3, we perform block CS reconstruction for above four test images with and without TV model, which is solved by split bregman algorithm. The parameter μ is related to the noise level, which is estimated by a robust median estimator based on mean absolute deviation as in [26]. The reconstruction images with and without postprocessing model at the sampling ratio of 0.3 are shown in Fig. 8 and the local details are zoomed in Fig. 9. From the Fig. 8, we can see that there are obvious blocking artifacts at the 16×16 grid caused by block structure used in the intra prediction and reconstruction noise in the reconstruction images without the postprocessing model. These artifacts and noises can be efficiently suppressed by our proposed postprocessing method based on TV model.

In order to evaluate the performance of our proposed algorithm compared with other classical algorithms, we reconstruct the above test images using three leading image compressed sensing reconstruction algorithms, including TVAL3[1], TwIST[2] and NESTA[3], and our proposed algorithm. All the algorithms used in our comparisons are

[1] http://www.caam.rice.edu/~optimization/L1/TVAL3/
[2] www.lx.it.pt/~bioucas/TwIST/TwIST.htm
[3] statweb.stanford.edu/~candes/nesta/

available from the corresponding author's website. We use the built-in parameter settings in each implementation which performed optimally. The measurement matrix Φ is implemented by the permutated Walsh-Hadamard transform [27]. All test images are divided into non-overlapping blocks of size 16×16. Fig. 10 displays their PSNR values with the growth of the measurement rate for each image. It can be seen that the proposed method performs best for all of the images at different sampling ratios.

As for the computational complexity about our proposed CS reconstruction algorithm compared with other general CS reconstruction algorithms, Our proposed CS reconstruction algorithm consists of three main modules, including ℓ_1 minimization solver, intra prediction and post-processing, so it is obvious that our proposed algorithm is more computational complex than the common CS reconstruction algorithms, which have only one ℓ_1 minimization solver module. However, it is not sensitive for CS image application because the increasing computation complexity is in the CS decoder rather than in the CS encoder.

5. Conclusion

In this article, we proposed a compressed sensing image reconstruction algorithm based on block-based compressed sensing framework for image application. The algorithm comprises of intra prediction, reconstruction of prediction residual and post-processing model. The current reconstruction block is firstly predicted by its surround neighbor reconstructed pixels, and the best intra prediction mode is selected in the CS measurement domain; secondly, instead of straightforward reconstructing the original image block as traditional CS, the prediction image residual block is reconstructed by some ℓ_1 convex optimization solvers, such as BPDN or GPSR etc. Furthermore, postprocessing method based on total variation model is also introduced to suppress the blocking artifacts caused by intra prediction and reconstruction noise caused by measurement error. Experimental results show that our proposed algorithm can significantly improve the performance of CS image. In the future work, more sophisticated intra prediction modes will be designed and integrated in our CS reconstructed algorithm to further improve its performance.

Acknowledgment

This work described in this article was supported by the Nation Natural Science Foundation of China (Grant No.61001123, 61379084, 61272323) and National Key Technology Research and Development Program of China (2012BAH06B01), and Hunan Province Science and Technology Planning Project (No. 2013FJ4033, 2014FJ6047 and 2014GK3030), and the Science Research Key Project of the Education Department of Hunan Province (No. 13A107).

References

[1] E. Cand`es, Compressive sampling, P. Int. Congress Mathematicians, Madrid, Spain 3 (2006) 1433–1452.
[2] D.L. Donoho, Compressed sensing, IEEE T. Inf. Theory 52 (4) (2006) 1289–1306 (September).
[3] J. Romberg, Imaging via compressive sampling [Introduction to compressive sampling and recovery via convex programming], IEEE Signal Proc. Mag 25 (2) (2008) 14–20 (March).
[4] E. Candès, J. Romberg, T. Tao, Robust uncertainty principles: Exact signal reconstruction from highly incomplete frequency information, IEEE T. Inf. Theory 52 (2) (2006) 489–509 (February).
[5] E. Candès, J. Romberg, T. Tao, Stable signal recovery from incomplete and inaccurate measurements, Comm. Pure Appl. Math 59 (8) (2006) 1207–1223.
[6] Stephen Boyd, Lieven Vandenberghe, Convex Optimization, Cambridge University Press, Cambridge, 2004.
[7] E. Candès, J. Romberg, l1-MAGIC:recovery of sparse signals via convex programming. ⟨http://www.acm.caltech.edu/l1magic/⟩.
[8] Ying Liu, Ming Li, D.A. Pados, Motion-aware decoding of compressed-sensed video, IEEE T. Circ. Syst. Vid 23 (3) (2013) 438–445 (March).
[9] S. Pudlewski, T. Melodia, A. Prasanna, Compressed-sensing enabled video streaming for wireless multimedia sensor networks, IEEE T. Mobile Comp 11 (6) (2011) 1060–1072 (June).
[10] Li Shang, D.S. Huang, Ji-Xiang Du, Chun-Hou Zheng, Palmprint recognition using FastICA algorithm and radial basis probabilistic neural network, Neurocomputing 69 (13–15) (2006) 1782–1786.
[11] Zhong-Qiu Zhao, D.S. Huang,, Bing-Yu Sun, Human face recognition based on multiple features using neural networks committee, Pattern Recogn. Lett 25 (12) (2004) 1351–1358.
[12] Xiao-Feng Wang, D.S. Huang,, Huan Xu, An efficient local Chan-Vese model for image segmentation, Pattern Recogn 43 (3) (2010) 603–618.
[13] Bo Li, D.S. Huang, Locally linear discriminant embedding: An efficient method for face recognition, Pattern Recogn 41 (12) (2008) 3813–3821.
[14] D.S Huang, Ji-Xiang Du, A constructive hybrid structure optimization methodology for radial basis probabilistic neural networks, IEEE T. Neural Netw 19 (12) (2008) 2099–2115.
[15] D.S Huang, Radial basis probabilistic neural networks: model and application, Int. J. Pattern Recogn. Artif. Intelligence 13 (7) (1999) 1083–1101.
[16] Xiao-Feng Wang, D.S. Huang, A novel density-based clustering framework by using level set method, IEEE T. Knowl. Data En 21 (11) (2009) 1515–1531.
[17] M.F. Duarte, M.A. Davenport, D. Takhar, J.N. Laska, T. Sun, K.F. Kelly, R.G. Baraniuk, Single-pixel imaging via compressive sampling, IEEE Signal Proc. Mag. 25 (2) (2008) 83–91 (March).
[18] J.E. Fowler, S. Mun, E.W. Tramel, Block-based compressed sensing of images and video, Found. Trends Signal Proc 4 (4) (2012) 297–416 (March).
[19] L. Gan, Block compressed sensing of natural images, in: Proceedings of the International Conference on Digital Signal Processing, Cardiff, UK, July 2007, 403–406.
[20] Jie Xu, Jianwei Ma, Dongming Zhang, Yongdong Zhang, Shouxun Lin, Improved total variation minimization method for compressive sensing by intra-prediction, Signal Proc. 92 (2012) 2614–2623.
[21] Z.-N. Li, M.S. Drew, Fundamentals of Multimedia, Pearson, Prentice-Hall, Upper Saddle River, NJ, 2004.
[22] I.E. Richardson, The H.264 Advanced Video Compression Standard, second ed., Wiley, New York, 2010.
[23] Signal and Image Processing Institute, University of Southern California, the USC-SIPI image database. ⟨http://sipi.usc.edu/database⟩, 2011. (Online).
[24] M.A.T. Figueiredo, R.D. Nowak, S.J. Wright, Gradient projection for sparse reconstruction: application to compressed sensing and other inverse problems, IEEE J. Sel. Area Comm 1 (4) (2007) 586–597 (December).
[25] T. Goldstein, S. Osher,, The split bregman method for l1-regularized problems, SIAM J. Imaging Sci 2 (2009) 323.
[26] D.L. Donoho, De-noising by soft-thresholding, IEEE T. Inform. Theory 41 (3) (1995) 613–627 (May).
[27] L. Gan,T. Do, T. Tran, Fast compressive imaging using scrambled block Hadamard ensemble, in: European Signal Processing Conference, Lausanne, Swithzerland, 2008.

Yun Song received his M.S. in computer application from Changsha University of Science & Technology, China in 2008. He is currently is an associate professor in the School of Computer and Communication Engineering of Changsha University of Science & Technology, China. And he is pursuing his PhD from Hunan University, China. His major research interests include video coding, multimedia communication and security, compressive video sensing, video analysis, and image processing.

Wei Cao received his M.S. in computer application from Hunan University, China. He is currently an assistant associate professor in the School of Computer and Communication Engineering of Changsha University of Science & Technology, China. His major research interests include video processing technology, multimedia technology, signal processing, pattern recognition, and image processing.

Yanfei Shen received the B.S. degree and the M.S. degree in computer science from the key laboratory of multimedia and network communication, Wuhan University, China, in 1999 and in 2002. He is currently working as associate researcher in Institute of Computing Technology, Chinese Academy of Sciences, Beijing, China. His research interests include video coding technology, video processing, digital TV, and associated VLSI architecture.

Gaobo Yang received his PhD in Communication Engineering from Shanghai University, China in 2004. He is currently a full professor in the School of Information Science & Engineering, Hunan University, China. He has published more than 40 papers in international journals and conferences. His research interests are in the area of multimedia communication, information security.